# **Cold Atmospheric Plasma Annealing of Plasmonic Silver Nanoparticles**

A. Sonawane<sup>a</sup>, M. A. Mujawar<sup>a</sup>, S. Bhansali<sup>a</sup>

<sup>a</sup> Department of Electrical and Computer Engineering, Florida International University, Miami, Florida 33173, USA

This work describes a new approach to anneal metallic nanoparticles at room temperature using atmospheric pressure plasma. Silver nanoparticle (AgNP) films were deposited on quartz substrates using aerosol injection technique. The AgNP films were annealed at 100°C - 400°C using rapid thermal processing, and at room temperature by cold atmospheric pressure plasma for 2 - 15 minutes. Surface plasmon resonance (SPR) of un-annealed AgNP films was observed at 426 nm, which was blue shifted by 5 to 70 nm after cold plasma annealing. The blue shift in SPR was also observed for thermally annealed AgNP films and the shift was similar to that of cold plasma annealing. SEM images showed the similar distribution of AgNPs on quartz substrates for both cold plasma annealed and thermally annealed AgNP films.

### Introduction

Surface plasmon resonance (SPR) is a unique optical property of metal nanoparticles which arises due to the interaction of electromagnetic waves with the conduction electrons on the nanoparticle surface. The collective oscillations of these conduction electrons at specific EM wavelengths leads to strong scattering and absorption. For silver nanoparticles (AgNP), the SPR occurs in UV-visible region and therefore AgNPs are used in various applications including solar energy harvesting, light emitting diodes, printed optoelectronic devices, and surface enhanced Raman scattering (SERS) (1). The SPR absorbance peak strongly depends on the size, shape, and assembly of the metal nanoparticles (2–4). The SPR absorbance peak can be tailored by thermal annealing of AgNPs (5). The annealing or sintering leads to change in mean diameter of nanoparticle due to nanoparticle agglomeration or reduction in the outer surface oxide layer of nanoparticles and therefore either red or blue shift in SPR is observed. However, thermal annealing is not always desirable, especially for the flexible polymer substrates in bio and environmental sensing applications.

In this paper, we report on the cold ( $\sim$ room temperature) atmospheric plasma annealing technique to study the effect of annealing parameters on optical properties of AgNPs deposited on silicon or SiO<sub>2</sub> substrates. The results are compared with the conventional rapid thermal processing at elevated temperatures. The scanning electron microscopy (SEM) is used to understand the nanoparticle morphology and their distribution on the substrates. UV-visible optical absorption spectroscopy is used to understand the effect of cold plasma / thermal annealing on the SPR. The results are compared to demonstrate the efficacy of cold atmospheric plasma annealing over thermal annealing.

## **Experimental Methods:**

## Cold Atmospheric Plasma

Figure 1 shows the schematic of the cold atmospheric plasma jet. The setup consists of a 6mm OD quartz tube on which two copper electrodes were placed 1 cm apart. The Ar gas flow was maintained at 2 l/min through the attached gas flow meter. The atmospheric plasma was produced by supplying the external high voltage electric field of 10kV to the copper electrodes. The high voltage supply was turned on and the impedance was adjusted such that the voltage supplied, and the variable frequency (~ 30 kHz) reached to the point where the plasma became stable. The voltage supply and gas flow were turned off after the treatment.

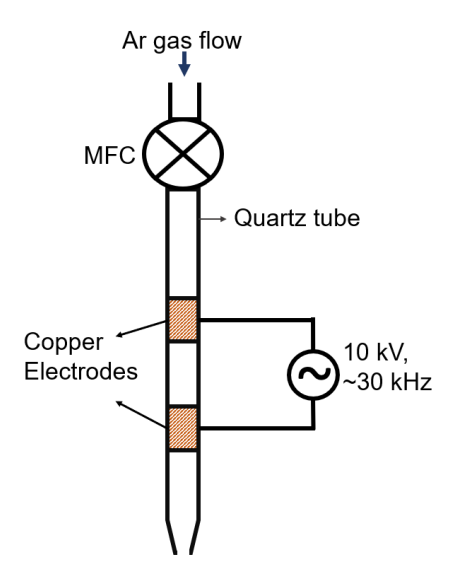


Figure 1: Schematic diagram of Plasma experimental setup

# **NPs Sintering**

The Ag NPs had an average size of 10 nm and were purchased from Sigma-Aldrich. A 0.02mg/ml solution of it was prepared in deionized water. The Ag NPs purchased were bi-polyethyleneimine (BPEI) functionalized to make the stable dispensed Ag NPs solution. Samples for SPR were prepared by depositing AgNPs on quartz slides followed by the plasma sintering for 5 minutes, 10 minutes, and 15 minutes. For the comparison between the plasma treated and thermally annealed substrates, sets of deposited slides were annealed using the RTP (Rapid Thermal Process) for the same interval of time at 250°C and 400°C. SPR signals were recorded for all samples using an Evolution 300 UV-Vis spectrometer from ThermoFisher.

#### **Results and Discussion**

Figures 2 (a) and (b) show the UV visible absorption spectra of AgNPs on SiO<sub>2</sub> substrate. For unannealed samples, the SPR peak was observed at a 426nm. This SPR peak shifted strongly towards blue after thermal and plasma annealing. The thermal annealing at 400°C for 10 mins resulted in the blue shift of SPR peak by of 28nm; while

for the 10 minutes of cold plasma annealing, the blueshift was of 37 nm. The absorbance peak intensity was observed to decrease after the cold plasma and thermal treatment.

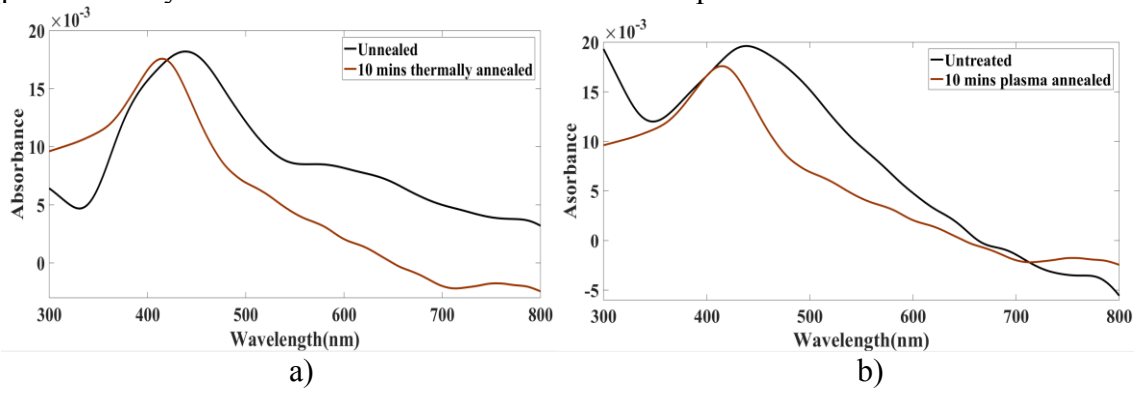


Figure 2: SPR absorbance of unannealed and a) 10 mins thermally annealed b) 10 mins plasma annealed Ag NPs films.

Figure 3 shows the plot of the blue shift in SPR after cold plasma annealing. The blue shift is 20nm, 37 nm and 70 nm for 5, 10 and 15 minutes of cold plasma treatment, and this shift is linear with respect to time. A similar trend was also observed for thermally annealed substrates. Moreover, the intensity of SPR absorbance was reduced for both cold plasma and thermally annealed samples.

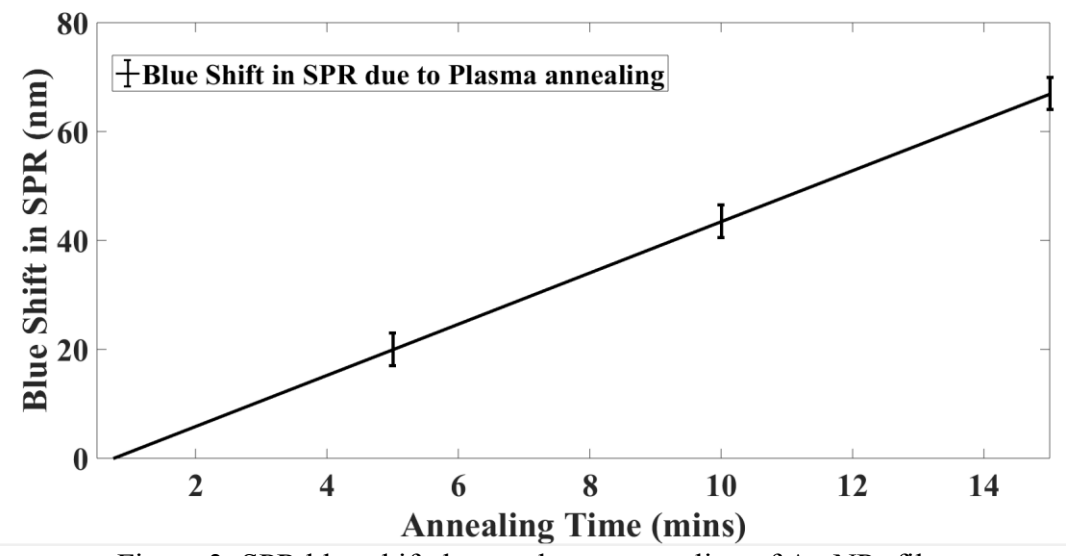


Figure 3: SPR blue shift due to plasma annealing of Ag NPs film

The AgNPs were deposited on silicon substrates and were annealed at room temperature and elevated temperatures using the same techniques which were used for the SPR study. Figures 4 (a) and (b) show the SEM images for untreated, and 10 minute plasma treated AgNPs on silicon substrates. From the SEM images, it was observed that the AgNPs' size was reduced. The distance between the particles increased and the particles were more organized and well dispersed after the treatments.

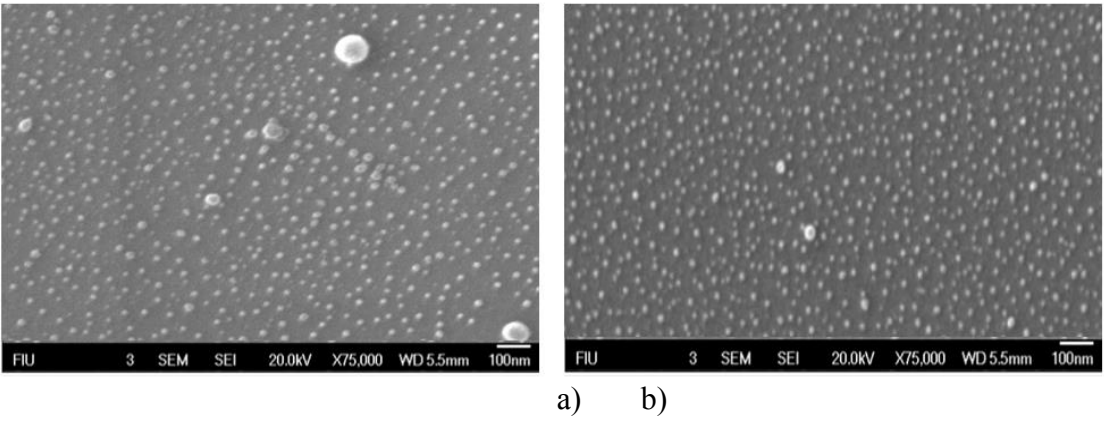


Figure 4: SEM image of a) unannealed and b) plasma annealed AgNPs film

The wavelength at which the SPR phenomenon occurs depends on the particle diameter, and a change in particle size accounts for a shift in the UV vis spectra towards either the blue or red range depending on whether the change in size is positive or negative (2,3,6). The UV-visible optical spectroscopy results showed that there was a blue shift in the SPR peak; which corresponded to the reduction in the AgNPs diameter after cold plasma and thermal treatment. The SEM images also confirmed this reduction in the nanoparticle diameter. The reduction in diameter after cold plasma and thermal annealing can be due to (i) the sublimation of surface oxide layer present on nanoparticle surfaces, and (ii) the disintegration and evaporation of BPEI organic coating on AgNPs. As the diameter of the AgNPs reduced, the surface to volume ratio was increased. This led to the increase in the number of scattering electrons on the surface of AgNPs which were responsible for the reduced lifetime of the oscillations and increased spectral width. This phenomenon of SPR peak widening was observed for both cold plasma treated and thermally annealed AgNPs films in figures 2 (a) and (b). The intensity of the SPR peak is dependent on both the concentration/density as well as the radius of the particles (7,8). Therefore, the reduction of peak intensity after treatment can be due to the increase in the distance between two adjacent nanoparticles and due to the reduction of the size of the NPs after sublimation of oxide layer on nanoparticles.

The Surface diffusion is dependent on the annealing temperature (9–11). Therefore, the increase in the temperature or plasma energy provided to the surface led to the activation of atoms and ultimately the diffusion on the surface. As the diffusion of deposited atoms took place, the activated atoms dispersed evenly, as seen in figures 4(a) and (b). The typical power supplied to create the cold plasma was on the orders of 1 W, which was much less than the power supplied to the RTP to create a temperature of 100 - 400°C. However, the nanoparticle distribution and SPR shift were more pronounced due to cold plasma annealing. In the case of thermal annealing, the entire sample surface was exposed to the heat energy, while in case of cold plasma treatment the energy was localized to a small area on the substrate surface. The concentration of plasma energy over a smaller surface led to the even diffusion and distribution of nanoparticles on the substrate.

### Conclusion

In summary, the effect of cold plasma annealing and thermal annealing of AgNP films were studied. Both the annealing techniques showed the blue shift in the SPR peak

of AgNPs. The results are explained by considering the annealing effects on the size reduction and dispersion of the nanoparticles. In case of cold plasma technique, the annealing effects are pronounced due to the concentration of plasma energy over a smaller region. This work has demonstrated the effectiveness of cold plasma annealing technique over thermal annealing and may found application in tailoring SERS substrates, biomaterial sintering, and nanofabrication of flexible electronics.

## Acknowledgments

This work is being supported by the NSF Nanosystems Engineering Research Centre for Advanced Self-Powered Systems of Integrated Biosensors and Technologies (ASSIST) under Award Number EEC-1160483 and NSF PFI-TT Award number 1827682.

#### References

- 1. A. E. Welles, *Silver Nanoparticles: Properties, Characterization and Applications*, (2010) http://www.sigmaaldrich.com/technical-documents/articles/materials-science/nanomaterials/silver-nanoparticles.html.
- 2. Y. Fleger and M. Rosenbluh, Res. Lett. Opt., 2009, 1–5 (2009).
- 3. K. B. Mogensen and K. Kneipp, J. Phys. Chem. C, 118, 28075–28083 (2014).
- 4. M. Kerker, D.-S. Wang, and H. Chew, *Appl. Opt.*, **19**, 3373–3388 (1980).
- 5. T. M. Khan et al., *Nanotechnology*, **28**, 445601 (2017).
- 6. W. Cai, H. Hofmeister, and T. Rainer, *Phys. E Low-Dimensional Syst. Nanostructures*, **11**, 339–344 (2001).
- 7. S. B. Wainhaus, E. A. Gislason, and L. Hanley, *J. Am. Chem. Soc.*, **119**, 4001–4007 (1997).
- 8. W. Haiss, N. T. K. Thanh, J. Aveyard, and D. G. Fernig, *Anal. Chem.*, **79**, 4215–4221 (2007).
- 9. M. Sui et al., Y. K. Mishra, Editor. *Appl. Surf. Sci.*, **416**, 1–13 (2017).
- 10. S. Y. Davydov, *Phys. Solid State*, **41**, 8–10 (1999).
- 11. L. T. Kong and L. J. Lewis, *Phys. Rev. B Condens. Matter Mater. Phys.*, **77**, 165422 (2008).